Characterization of supported rhenium oxide catalysts: effect of loading, support and additives

Brishti Mitra,[a] Xingtao Gao,[b] Israel E. Wachs,[b] A. M. Hirt[c] and Goutam Deo*[a]

[a] Department of Chemical Engineering, Indian Institute of Technology, Kanpur 208 016, India.
E-mail: goutam@iitk.ac.in
[b] Zettlemoyer Center for Surface Studies and Department of Chemical Engineering, Lehigh University, Bethlehem, PA 18015, USA
[c] Materials Research Laboratory, Inc., 290 North Bridge Street, Struthers, OH 44471, USA

The nature of the surface rhenium oxide species present in supported rhenium oxide catalysts was determined as a function of the oxide support, rhenium oxide loading and secondary metal oxide additives. The catalysts were prepared using the incipient wetness impregnation method with dilute aqueous perrhenic acid as the precursor and characterized using Raman, FTIR and X-ray photoelectron spectroscopy (XPS) and temperature programmed reduction (TPR) experiments. The Raman and XPS studies reveal that the surface rhenium oxide species are well dispersed on the Al_2O_3 and TiO_2 supports. Under dehydrated conditions, Raman and IR studies reveal that the surface rhenium oxide species is independent of oxide support (Al_2O_3 and TiO_2) and it appears that the same isolated rhenium oxide species is formed for all loadings. The structural details of this dehydrated isolated rhenium oxide species are, however, not clear. TPR measurements suggest that the reducibility of the surface rhenium oxide species depends strongly on the specific oxide support: the surface rhenium oxide species on TiO_2 is more reducible than the surface rhenium oxide species on Al_2O_3. The difference in reducibility is related to the bridging Re–O–support bond strength. The secondary metal oxide additives, sodium and vanadium, can be categorized as interacting and non-interacting, respectively. The non-interacting additive (vanadium oxide) coordinates directly to the oxide supports without significantly affecting the structure and reducibility of the surface rhenium oxide species. The interacting additive (sodium oxide), however, directly coordinates with the surface rhenium oxide species and changes its structure and hydrogen reducibility.

Introduction

Supported metal oxide systems constitute a very important class of heterogeneous catalysts. These catalysts are formed when a metal oxide is deposited on the surface of a second metal oxide substrate that usually possesses a high surface area.[1–3] The deposited metal oxide component is considered to be the active phase of the catalyst and some of the reported active oxides are those of vanadium, rhenium, chromium, molybdenum, niobium, tungsten, etc. The typical high surface area metal oxide supports used are alumina, titania, silica, zirconia, niobia, etc. These supported metal oxide catalysts find numerous applications in the petrochemical industry and for pollution control.[4]

Supported rhenium oxide catalysts belong to this group of supported metal oxide catalysts. In such catalysts the active rhenium oxide component forms a two-dimensional overlayer on oxide supports. The importance of these catalysts lies in their extensive use for the metathesis of olefins.[5–7] Olefin metathesis or olefin disproportionation reactions are industrially very important. These reactions provide an alternative way of producing useful compounds that cannot be synthesized from readily available starting materials by standard methods.[8,9] Tungsten oxide and molybdenum oxide catalysts are also employed for metathesis of olefins, but rhenium oxide is superior under mild reaction conditions, viz., room temperature and atmospheric pressure. These conditions help reduce side reactions such as isomerization and poly-merization, yielding exclusively the primary metathesis products.[9] Rhenium based catalysts have also been examined for hydrodesulfurization,[10,11] hydrodenitrogenation,[12] selective hydrogenation,[13] selective catalytic reduction of NO_x[14] and partial oxidation of methanol.[15] The catalytic activity of the supported rhenium oxide catalysts for metathesis is enhanced by the presence of other metal oxides additives, such as V_2O_5, MoO_3 and WO_3,[16,17] and by the use of mixed oxide supports such as $SiO_2 \cdot Al_2O_3$ and $Al_2O_3 \cdot B_2O_3$.[17–19] Addition of MR_4 (M = Sn or Pb; R = alkyl) also helps in improving the activity of supported rhenium oxide catalysts.[17–20]

The industrial importance of the supported rhenium oxide catalysts has motivated fundamental studies about the nature and function of the active sites in such catalysts, namely the surface rhenium oxide species present. Knowledge of the surface composition and the local structure of the catalyst at the molecular level will help in understanding better the role played by the surface species in the catalytic reactions. The molecular-level information can then be used to assist in the design of improved catalysts. The surface rhenium oxide over-layer in the supported rhenium oxide catalysts has been characterized by extended X-ray absorption fine structure (EXAFS),[21] X-ray absorption near edge spectroscopy (XANES),[21,22] Fourier transform infrared (FTIR) spectroscopy,[23–25] UV–visible spectrophotometry[23] and Raman spectroscopy.[20,22–24,26,27] Of these characterization techniques, Raman spectroscopy is best suited for the study of supported metal oxide catalysts and, consequently, supported rhenium

oxide catalysts. The molecular nature of this characterization technique and its ability to discriminate between different metal oxide species that may simultaneously be present in the catalyst make Raman spectroscopy a very powerful characterization tool.[28,29] IR spectroscopic studies are also very useful, but most of these studies are hampered by the absorption by the oxide support that obscures many of the metal–oxygen vibrations. IR spectroscopy can, however, detect those vibrations that are not Raman active due to the highly ionic nature of the bond in regions not obscured by absorption of the oxide support (greater than ~ 1000 cm^{-1}). Raman and IR spectroscopy also have the advantage of being carried out under *in situ* conditions. X-ray photoelectron spectroscopy (XPS) helps in providing information about the dispersion and the oxidation state of rhenium oxide species on oxide support surfaces.[30–34] The reduction properties of the supported rhenium oxide catalysts that are important for redox reactions can be determined by the temperature programmed reduction (TPR) technique and have been employed in several investigations.[24,35–37]

Acquiring fundamental information about supported metal oxide catalysts requires that the surface metal oxide species be a well-defined system, *i.e.*, knowledge of the structure and support interactions is necessary. Based on the above-mentioned research, it is evident that the surface rhenium oxide species is ideally suited for fundamental studies involving supported metal oxide catalysts. This is so since previous studies suggest that the surface rhenium oxide species is isolated[24] and complications occurring due to multiple, polymeric and ill-defined species do not arise. Furthermore, there appears to be a lack of characterization studies on the effect of additives on supported rhenium oxide catalysts, which should assist in enhancing the knowledge of the structure and support interaction of the surface rhenium oxide species. Thus, to address these issues, the objectives of the present work were broadly classified as (i) synthesis of the surface rhenium oxide species on Al$_2$O$_3$ and TiO$_2$ supports, (ii) characterization of the surface rhenium oxide species as a function of oxide support (Al$_2$O$_3$ and TiO$_2$), rhenium oxide loading and additives (oxides of vanadium and sodium) and (iii) the influence of the above parameters on the nature of the surface rhenium oxide species.

Experimental

Preparation of catalyst samples

The supported rhenium oxide catalysts were prepared by the incipient wetness impregnation technique. The precursor used was a 60–70% aqueous solution of perrhenic acid (HReO$_4$) (Aldrich, 99.98% purity) and the supports used were titania (Degussa P-25, 55 m^2 g^{-1}) and alumina (Harshaw, 180 m^2 g^{-1}). The supports were pre-treated with incipient volumes of doubly distilled water and then calcined at 450 °C (TiO$_2$) or 500 °C (Al$_2$O$_3$) for 16 h. The supports and the incipient volumes of perrhenic acid solution were then intimately mixed. The samples were dried at room temperature for 16 h, followed by drying at 110 °C for 7 h and at 200 °C for 16 h. Finally, the Re$_2$O$_7$/TiO$_2$ and Re$_2$O$_7$/Al$_2$O$_3$ samples were calcined at 450 and 500 °C for 2 h, respectively. The final catalysts were denoted as x% Re$_2$O$_7$/support, where x% denotes the weight per cent of Re$_2$O$_7$ per unit weight of total catalyst.

The effect of two different types of metal oxide additives, sodium and vanadium, on the surface rhenium oxide species was investigated. For the first type of additive, known amounts of sodium hydroxide (NaOH, 20% solution) were added to previously prepared 3.1% Re$_2$O$_7$/TiO$_2$ or 7.8% Re$_2$O$_7$/Al$_2$O$_3$ samples as described above. In the second type of additive, known amounts of perrhenic acid solution were added to previously prepared 1% V$_2$O$_5$/TiO$_2$ and 1%

V$_2$O$_5$/Al$_2$O$_3$ samples as described previously.[38] Doubly distilled water was added to an NaOH and an HReO$_4$ solution separately to form incipient wetness volumes of the two solutions. The incipient wetness volumes of the two solutions were added to the 3.1% Re$_2$O$_7$/TiO$_2$, 7.8% Re$_2$O$_7$/Al$_2$O$_3$, 1% V$_2$O$_5$/TiO$_2$ or 1% V$_2$O$_5$/Al$_2$O$_3$ samples. The drying and heating of the samples were performed under conditions similar to those for the supported rhenium oxide samples as described above. The samples were denoted as follows: y% Na$_2$O/3.1% Re$_2$O$_7$/TiO$_2$ or y% Na$_2$O/7.8% Re$_2$O$_7$/Al$_2$O$_3$, where y% is the weight per cent of Na$_2$O deposited based on the total weight of the sample, and z% Re$_2$O$_7$/1% V$_2$O$_5$/TiO$_2$ (or Al$_2$O$_3$), where z% denotes the weight per cent of Re$_2$O$_7$ deposited based on the total weight of the sample.

Rhenium determination

The actual rhenium oxide loadings for the supported rhenium oxide catalysts were determined by atomic absorption spectroscopy (AAS) using an AAnalyst 300 (Perkin-Elmer) spectrometer. A 200 mg amount of the sample was dissolved in about 2 ml of concentrated sulfuric acid and 20 ml of distilled water. This was evaporated for 1.5 h, filtered and then water was added to make 100 ml of solution. Potassium perrhennate was used as a standard and a rhenium lamp source was used to determine the rhenium content actually present.

X-ray photoelectron spectroscopy (XPS) studies

The near surface compositions of the Re$_2$O$_7$/TiO$_2$ and Re$_2$O$_7$/Al$_2$O$_3$ samples were determined using XPS. A beam of predominantly Mg Kα or Al Kα X-rays was used for this analysis. The electron spectrometer was operated in the fixed analyzer transmission (FAT) mode. Additional details can be found elsewhere.[39] The XPS surface analyses were performed on samples exposed to ambient conditions and, consequently, were hydrated.

Raman spectroscopy studies

The laser Raman spectra of the supported rhenium oxide catalysts with and without additives under ambient and dehydrated conditions were obtained by means of an argon ion laser (Spectra Physics, Model 165). Details of the Raman spectrometer can be found elsewhere.[40,41] About 200 mg of the supported rhenium oxide catalysts were pressed into self-supporting wafers and placed in a rotating sample cell, to avoid local heating effects. For obtaining the dehydrated Raman spectra of the unmodified supported rhenium oxide samples, the rotating *in situ* Raman cell developed by Jehng *et al.*[40] was used. The cell was gradually heated at 400 °C and kept at this temperature for 1 h and the Raman spectrum was obtained. The entire procedure was performed in a stream of flowing oxygen (ultra high purity grade Linde gas) over the catalyst samples to ensure complete oxidation of the catalysts. For obtaining the Raman spectra of the supported rhenium oxide samples with additives under dehydrated conditions, the Raman cell and procedure described by Vuurman *et al.*[24] was used.

Fourier transform infrared (FTIR) studies

The FTIR spectra of Re$_2$O$_7$/TiO$_2$ and Re$_2$O$_7$/Al$_2$O$_3$ under dehydrated conditions were recorded on a Bio-Rad FTS-7 spectrometer (resolution 2 cm^{-1} and accuracy in the peak position ~ 2 cm^{-1}). The samples were pressed into self-supporting wafers (30–40 mg cm^{-2}) and mounted on an *in situ* IR cell developed by Burcham and Wachs.[42] Initially, pure oxygen was flowed over the sample as the temperature was increased to 300 °C and maintained for 1 h. Two spectra were taken at intervals of 1 h to check whether they were identical.

Temperature programmed reduction (TPR) studies

TPR studies were carried out on the supported rhenium oxide samples with and without additives. A mixture of 10% hydrogen–argon at 1 bar pressure was used in a TPR apparatus (Altamira Instruments, Model AMI-100). The weight of the sample varied from 5 to 100 mg. Various runs were carried out on a particular sample with decreasing sample weight in order to eliminate errors due to mass transfer limitations. The samples were precalcined *in situ* at 500 °C in air for 15 min in order to dehydrate the samples. The samples were then cooled to 50 °C and dry argon was flushed to remove the air. A mixture of hydrogen and argon in a molar ratio of 1 : 9 was then passed at a flow rate of 17 μmol s^{-1}. TPR measurements were carried out by increasing the temperature linearly at the rate of 10 °C min^{-1} up to 600 °C. The hydrogen consumption was monitored quantitatively using a thermal conductivity detector.

Results

The supported rhenium oxide samples were analyzed for actual Re_2O_7 loadings by AAS and the actual loadings are presented in Table 1. Also included in Table 1 is the actual rhenium concentration per unit surface area (Re atoms nm^{-2}). The loadings of rhenium, vanadia and sodium in the modified supported rhenium oxide samples are presented in Table 2. Table 2 also contains the atomic ratios of additive to rhenium, *i.e.*, A/Re, where A = V or Na.

XPS studies

The Re_2O_7/Al_2O_3 and Re_2O_7/TiO_2 catalysts were examined by XPS. From XPS analysis, the surface atomic concentrations of Re and S (S = Al or Ti) are obtained and the Re/S atomic ratio is calculated. The XPS-determined Re/S atomic ratios, $(Re/S)_{XPS}$, are plotted *vs.* the bulk atomic ratio, $(Re/S)_{bulk}$, in Fig. 1. The $(Re/S)_{XPS}$ *vs.* $(Re/S)_{bulk}$ plots exhibit a linear dependence, which reflects the highly dispersed nature of the supported rhenium oxide phase on the surface of the

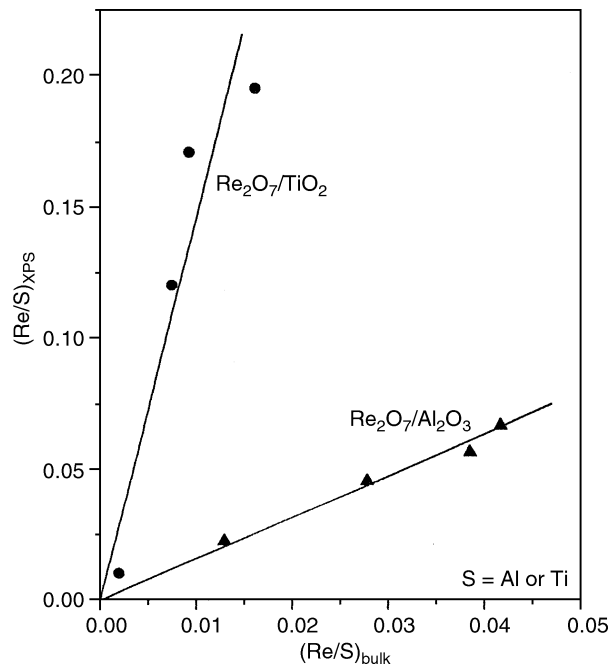**Fig. 1** Ratio of Re/S as measured by XPS to that present in the bulk, where S = Al or Ti.

oxide supports. Furthermore, the slope of the $(Re/Ti)_{XPS}$ *vs.* $(Re/Ti)_{bulk}$ line is greater than that of the $(Re/Al)_{XPS}$ *vs.* $(Re/Al)_{bulk}$ line.

Raman spectroscopy studies

The Raman spectra were initially obtained under ambient conditions and then under dehydrated conditions. However, the Raman spectra are not shown since they are similar to previously published spectra.[24] The ambient Raman spectra revealed the presence of isolated ReO_4^- species (strong band at 977–991 cm^{-1} and weak band at $\sim$920 cm^{-1}) irrespective of the support and rhenium oxide loading, which is in agreement with previous studies.[24]

The dehydrated Raman spectra of the 4.1–11.3% Re_2O_7/Al_2O_3 samples in the 600–1200 cm^{-1} region reveal a sharp Raman band at $\sim$1000 cm^{-1} for all the samples. An additional Raman band at 973 cm^{-1} is observed for the 10.1 and 11.3% Re_2O_7/Al_2O_3 catalysts. The Raman band at $\sim$1000 cm^{-1} increases in intensity with increasing rhenium oxide loading. Raman bands similar to the $\sim$1000 and 973 cm^{-1} bands were observed previously by Vuurman *et al.*,[24] and were assigned to the symmetric and asymmetric stretching modes of terminal Re=O bonds, respectively.

The dehydrated Raman spectra of the 0.7–4.8% Re_2O_7/TiO_2 samples in the 700–1100 cm^{-1} region reveal a strong band at 1003 cm^{-1} for catalysts of all rhenium oxide loadings. This peak is assigned to the symmetric stretching mode of the surface rhenium oxide species. The asymmetric stretching mode expected at lower wavenumbers, however, is not clearly discernible. Similarly to the Re_2O_7/Al_2O_3 system, the symmetric stretching band at 1003 cm^{-1} increases in intensity with increasing rhenium oxide loading.

FTIR spectroscopy studies

The FTIR spectra of the supported rhenium oxide samples were obtained only under dehydrated conditions since under ambient conditions the bands of water and carbon dioxide interfere with the metal oxide bands under these conditions. The dehydrated FTIR spectra are not shown for brevity and are similar to previously published spectra.[24] The dehydrated

Table 1 Actual rhenium oxide loading on TiO_2 and Al_2O_3 supports

Oxide support	Re_2O_7 loading (wt.%)	Re surface concentration/ atoms nm^{-2}
TiO_2	0.7	0.32
	2.5	1.13
	3.1	1.40
	4.8	2.17
Al_2O_3	4.1	0.57
	7.8	1.08
	10.1	1.39
	11.3	1.56

Table 2 Amount of additives (A) used and A/Re atomic ratio present

Sample	Re_2O_7 loading (wt.%)	V_2O_5 loading (wt.%)	Na_2O loading (wt.%)	A/Re atomic ratio
Re–V–Ti	2.9	1	—	0.9
Re–V–Al	4.5	1	—	0.57
	7.3	1	—	0.34
Re–Na–Ti	3.1	—	1	2.47
	3.1	—	2	4.98
	3.1	—	3	7.55
Re–Na–Al	7.8	—	1	0.93
	7.8	—	5	4.86
	7.8	—	10	10.26

IR spectra of the 4.1–11.3% Re_2O_7/Al_2O_3 samples in the first overtone region reveal the presence of two prominent bands at 1988–1992 and 1954 cm^{-1}, which are assigned to the symmetric and asymmetric vibrations of the Re=O vibrations. In the case of IR spectra, the asymmetric vibration is stronger than the symmetric vibration owing to the larger dipole change involved. Accordingly, the 1954 cm^{-1} peak (asymmetric stretching band) is more intense than the $\sim$1990 cm^{-1} band. The band positions are, however, not exactly double the values of the fundamental bands at 1000 and 973 cm^{-1} owing to the anharmonicity of the Re=O vibrations.[24] The intensity ratio of the two IR bands appeared not to change with increasing rhenium oxide loading.

The dehydrated IR spectra for 0.7–4.8% Re_2O_7/TiO_2 samples in the 1800–2100 cm^{-1} region reveal two prominent bands at 2001–2004 and 1966–1974 cm^{-1} similar to the Re_2O_7/Al_2O_3 system. As before, the 2001–2004 and 1966–1974 cm^{-1} bands correspond to the symmetric and asymmetric vibrations, respectively. However, the intensity ratio of the two bands for the 0.7% Re_2O_7/TiO_2 sample is different from the 4.8% Re_2O_7/Al_2O_3 sample, suggesting that subtle differences between the surface rhenium oxide species exist. It is worth noting that the 1974 cm^{-1} band corresponding to the asymmetric stretching mode, which is absent in the Raman spectra, is clearly observed in the IR spectra.

The hydroxyl regions of the different supported rhenium oxide samples were also studied by FTIR spectroscopy and the support hydroxyl bands (for Al_2O_3 support, 3727, 3675 and 3563 cm^{-1}, and for TiO_2 support, 3720, 3662, 3630 and $\sim$3490 cm^{-1}) were observed to decrease with an increase in rhenium oxide loading. This is consistent with previous studies.[43]

Temperature programmed reduction studies

The TPR profiles for the 4.1–11.3% Re_2O_7/Al_2O_3 samples revealed a single sharp reduction peak for all rhenium oxide loadings. The TPR peak maximum is similar for all loadings and lies in the 337–361 °C range, which is within experimental variations. This observation for the Re_2O_7/TiO_2 samples is consistent with the study of Okal et al.,[44] where oxidation of rhenium metal on Al_2O_3 was observed at temperatures greater than 300 °C. The TPR patterns for the 0.7–4.8% Re_2O_7/TiO_2 samples also revealed a sharp reduction peak similar to the Re_2O_7/Al_2O_3 samples. However, the TPR peak maximum lies in the 191–237 °C range. The TPR peak maxima of the Re_2O_7/Al_2O_3 and Re_2O_7/TiO_2 samples are plotted vs. surface rhenium concentration (Re atoms nm^{-2}) in Fig. 2.

A quantitative analysis of the TPR results for Re_2O_7/TiO_2 and Re_2O_7/Al_2O_3 catalysts was also performed. The number hydrogen atoms required per rhenium atom reduced for different supported rhenium oxide samples indicates that the reduction of the Re is from the +7 oxidation state to the zero valence state (Re metal), irrespective of the specific oxide support and the rhenium oxide loading.

Effect of additives

Rhenia–vanadia–titania and rhenia–vanadia–alumina catalysts. The dehydrated Raman spectrum of 2.9% $Re_2O_7/1\%$ V_2O_5/TiO_2 is shown in Fig. 3 in the 700–1100 cm^{-1} region. The spectra of 1% V_2O_5/TiO_2 and 3.1% Re_2O_7/TiO_2 are included for comparison. As discussed before, the spectrum of the 3.1% Re_2O_7/TiO_2 sample exhibits a band at 1003 cm^{-1} due to the Re=O vibration. The Raman spectrum of the 1% V_2O_5/TiO_2 catalyst exhibits a band at 1026 cm^{-1} due to the V=O vibration.[45] A distinct band at $\sim$1003 cm^{-1} is observed for the 2.9% $Re_2O_7/1\%$ V_2O_5/TiO_2 samples that is similar to that for the Re_2O_7/TiO_2 sample. The rhenia–vanadia–titania
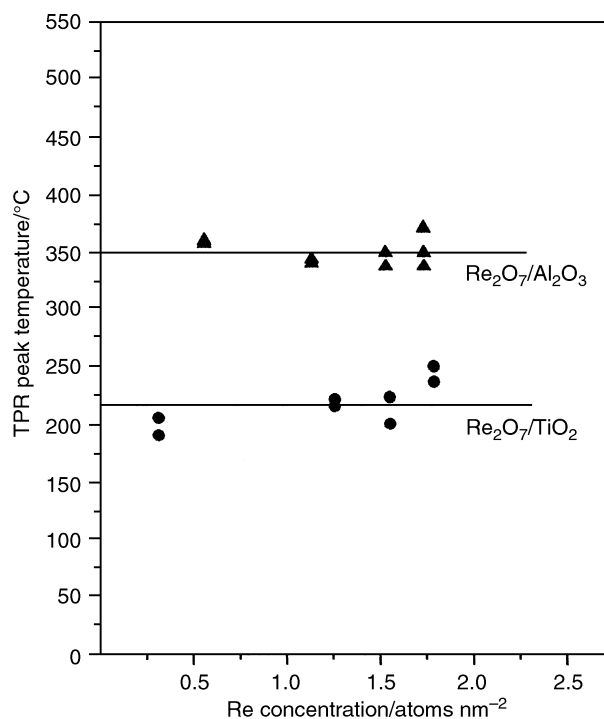
Fig. 2 Reduction peaks for the different Re_2O_7/Al_2O_3 and Re_2O_7/TiO_2 samples as a function of rhenium oxide loading.

spectrum, however, does not clearly show Raman features due to vanadium–oxygen vibrations. The presence of the surface vanadium oxide species in the 2.9% $Re_2O_7/1\%$ V_2O_5/TiO_2 Raman spectrum can be observed as a slight shoulder at $\sim$1025 cm^{-1}. There is a weak band around 796 cm^{-1} for all spectra, which is due to the titanium–oxygen vibration from the TiO_2 support.[46]
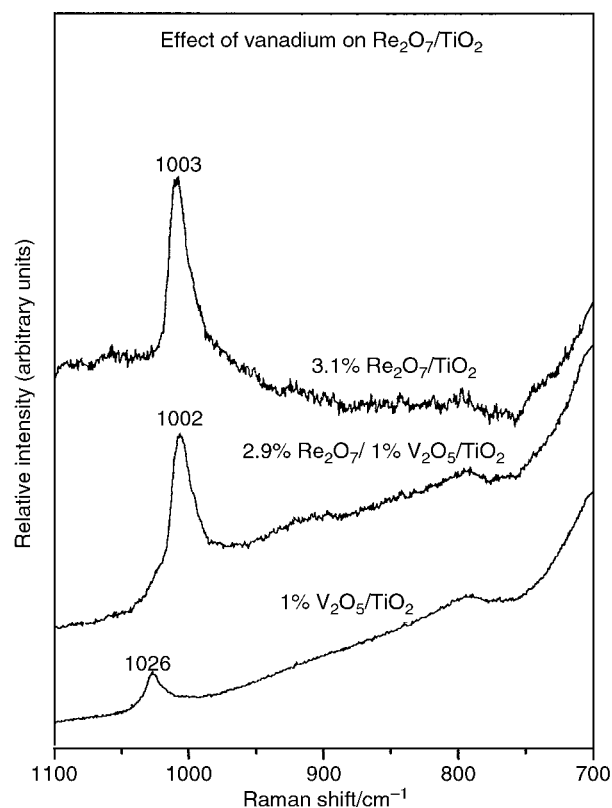

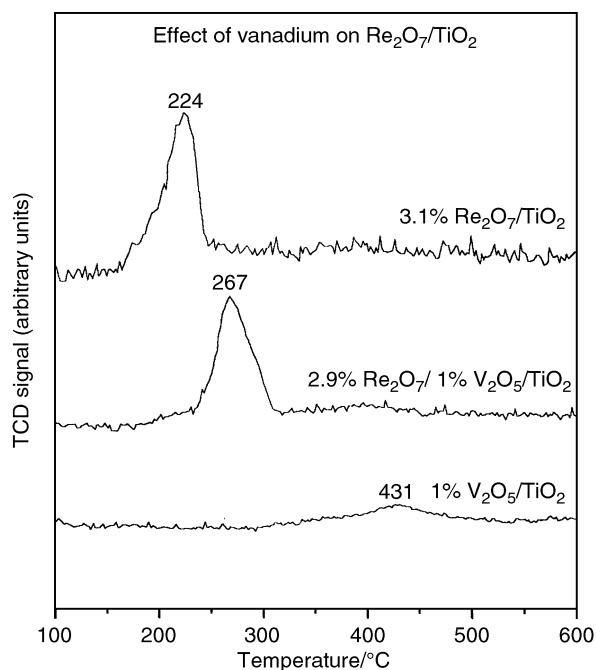**Fig. 3** Raman spectra of vanadium doped Re_2O_7/TiO_2. Spectra obtained under dehydrated conditions.

Fig. 4 TPR profile of vanadium doped Re_2O_7/TiO_2.

Fig. 5 TPR profile of vanadium doped Re_2O_7/Al_2O_3.

The TPR pattern for the vanadium oxide modified Re_2O_7/TiO_2 catalyst is presented in Fig. 4. The sample shows a well-defined reduction peak at 267 °C. The TPR data for 1% V_2O_5/TiO_2 and 3.1% Re_2O_7/TiO_2 have been included for comparison. The TPR peak maximum for the 3.1% Re_2O_7/TiO_2 samples is at 224 °C and that for the 2.9% $Re_2O_7/1\%$ V_2O_5/TiO_2 sample is at 267 °C. The TPR peak for the 1% V_2O_5/TiO_2 is at a much higher value of 431 °C. No reduction peaks in this region are observed for the rhenia–vanadia–titania sample. In the presence of surface vanadium oxide, however, the reduction peak of surface rhenium oxide has shifted to a slightly higher value, which implies that the reducibility of the surface rhenium oxide species is slightly affected. However, no significant difference in the amount of hydrogen consumed per rhenium is observed.

The dehydrated Raman spectra of vanadium oxide doped Re_2O_7/Al_2O_3 catalyst could not be obtained owing to fluorescence problems. However, by comparison with the $V_2O_5/Re_2O_7/TiO_2$ system, the Raman spectra of $V_2O_5/Re_2O_7/Al_2O_3$ should be similar to that of Re_2O_7/Al_2O_3.

The TPR profile for the vanadium oxide modified Re_2O_7/Al_2O_3 samples is shown in Fig. 5. The patterns for 1% V_2O_5/Al_2O_3, 4.1% Re_2O_7/Al_2O_3 and 7.8% Re_2O_7/Al_2O_3 are included for comparison. Whereas the other four samples show an intense single reduction peak at 340–371 °C, the reduction peak at 530 °C for 1% V_2O_5/Al_2O_3 is hardly visible. Similarly to the previous case with the rhenia–vanadia–titania catalyst, the reduction peaks of surface rhenium oxide have shifted to a slightly higher values owing to the presence of the surface vanadium oxide species. Furthermore, the amount of hydrogen consumed per rhenium remains the same.

Sodium–rhenia–titania and sodium–rhenia–alumina catalysts. The Raman spectra of sodium modified Re_2O_7/Al_2O_3 and Re_2O_7/TiO_2 samples were obtained under ambient and dehydrated conditions. The ambient Raman spectra of the $x\%$ $Na_2O/3.1\%$ Re_2O_7/TiO_2 samples (not shown) reveals bands at $\sim$970, $\sim$958, $\sim$924 and $\sim$888 cm^{-1}. The Raman bands at 958, 924, 888 cm^{-1}, which are not observed for unmodified Re_2O_7/TiO_2 samples, are observed to increase with increase in sodium loading. The dehydrated Raman
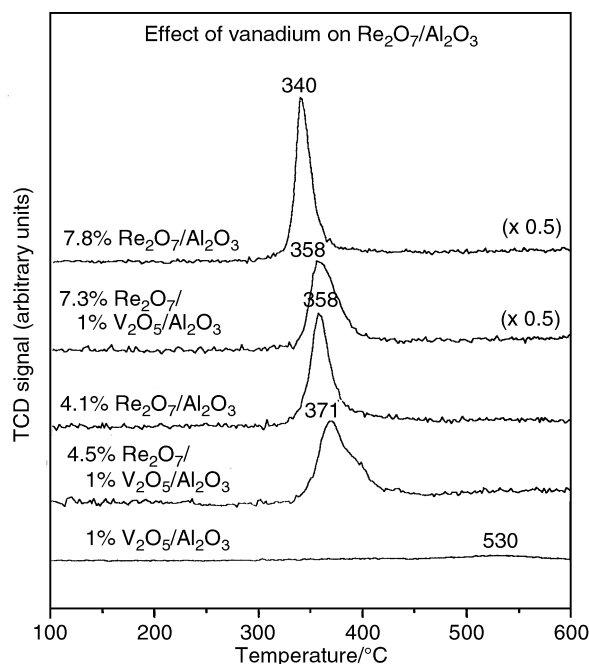
spectra for different sodium loadings (as Na_2O) on 3.1% Re_2O_7/TiO_2 in the 750–1100 cm^{-1} region are shown in Fig. 6. For the 3.1% Re_2O_7/TiO_2 sample, the Raman band is at 1003 cm^{-1}. On adding 1–3% Na_2O, distinct Raman bands are observed at $\sim$975 cm^{-1} and a broad band develops at $\sim$888 cm^{-1}.

The TPR patterns for the sodium modified Re_2O_7/TiO_2 catalysts are presented in Fig. 7. All samples show a well-defined reduction peak at 401–433 °C. The TPR data for 3.1% Re_2O_7/TiO_2 have been included for comparison. The reduction peak for the 3.1% Re_2O_7/TiO_2 samples occurs at 224 °C, which is very different from the reduction peak of the sodium–rhenia–titania samples observed at 401–433 °C. The
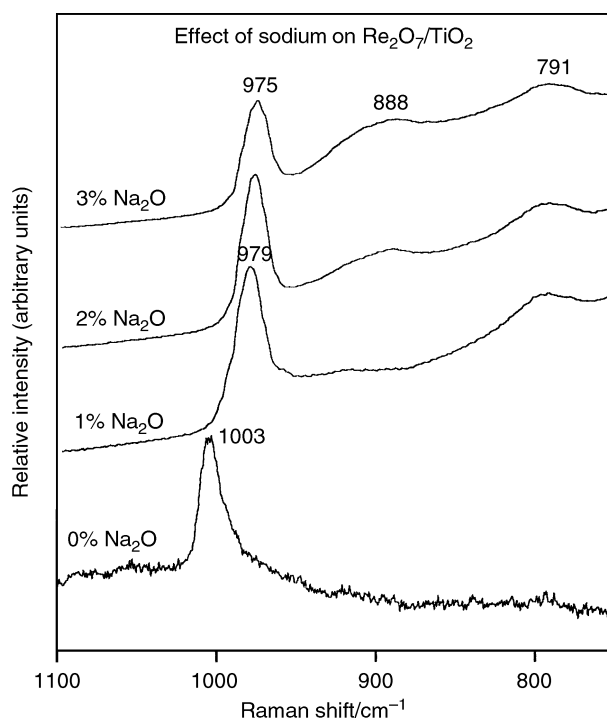

Fig. 6 Raman spectra of sodium doped Re_2O_7/TiO_2. Spectra obtained under dehydrated conditions.

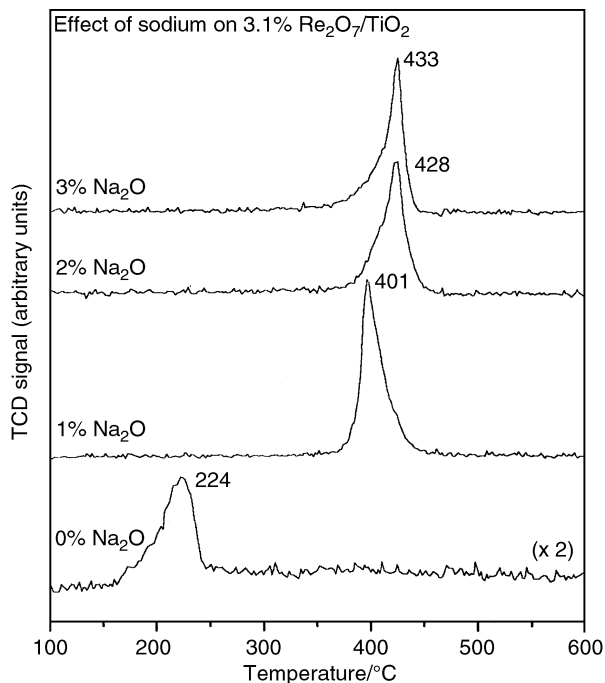**Fig. 7** TPR profile of sodium doped Re_2O_7/TiO_2.

Fig. 9 TPR profile of sodium doped Re_2O_7/Al_2O_3.

amount of hydrogen consumed does not change with increase in the sodium content in the sodium modified Re_2O_7/TiO_2 samples.

The ambient Raman spectra of the $x\%$ $Na_2O/7.8\%$ Re_2O_7/Al_2O_3 samples (not shown) reveal bands at ~ 970, ~ 924 and 335 cm^{-1}. The dehydrated Raman spectra for different sodium loadings (as Na_2O) on 7.8% Re_2O_7/Al_2O_3 in the 200–1100 cm^{-1} region are shown in Fig. 8. For the 1% $Na_2O/7.8\%$ Re_2O_7/Al_2O_3 sample the Raman band is at 1002 and 335 cm^{-1}. On adding 5 or 10% Na_2O to the 7.8%
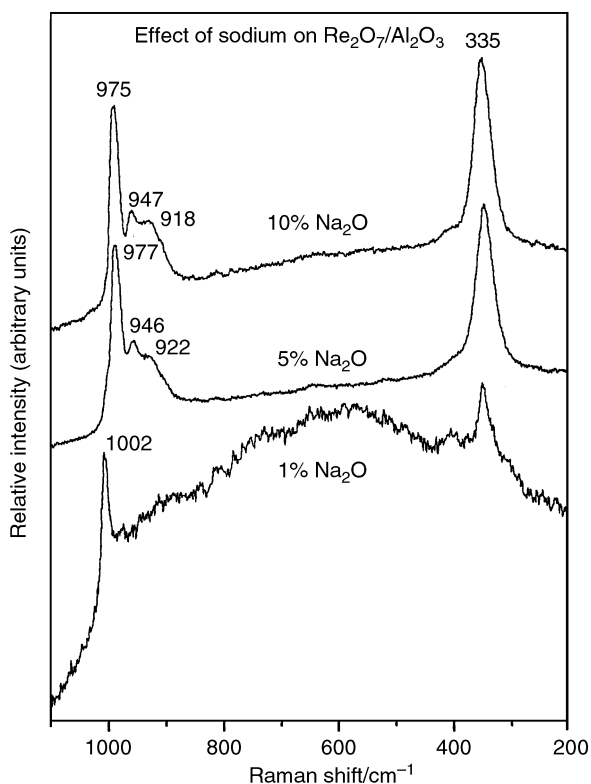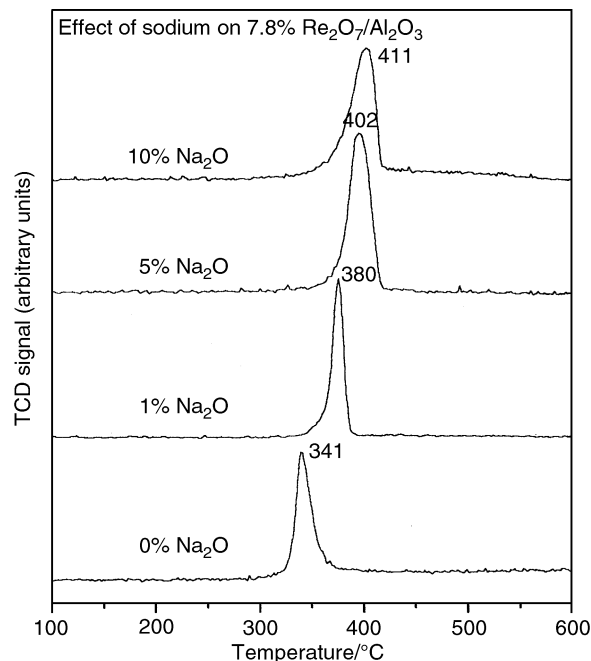
Re_2O_7/Al_2O_3 sample, sharp Raman bands are observed at 977–975 cm^{-1} with weak bands at ~ 947 and ~ 920 cm^{-1}. The Raman band at 335 cm^{-1} is still present.

The TPR patterns for the sodium doped 7.8% Re_2O_7/Al_2O_3 catalysts are presented in Fig. 9. All samples show a well-defined reduction peak whose position increases from 380 to 411 °C with an increase in sodium addition from 1 to 10% Na_2O. The TPR data for 7.8% Re_2O_7/Al_2O_3 have been included for comparison. The reduction peak for the 7.8% Re_2O_7/Al_2O_3 sample occurs at 341 °C, which is much lower than the temperature of the reduction peak of the sodium–rhenia–alumina samples at 380–411 °C. Similarly to the previous samples, the amount of hydrogen consumed does not change significantly with the presence of sodium.

Discussion

It is known that the surface rhenium oxide species is extremely volatile.[22] This is related to the volatility of bulk Re_2O_7 and the formation of dimeric Re_2O_7 gaseous species. At elevated temperatures, as soon as two surface species come into close proximity, they combine to form a gaseous Re_2O_7 molecule that desorbs from the surface. Volatility of the deposited rhenium oxide species is possible since preparation of the supported rhenium oxide requires final calcination at 450–500 °C. It is therefore important to determine the actual rhenium content on the surface. This is achieved by analyzing the various supported rhenium oxide samples prepared for the actual rhenium content by AAS. Once the actual rhenium oxide content has been determined, the rhenium oxide species in the various samples can be studied using the different characterization techniques.

Effect of oxide support and rhenium oxide loading

XPS studies. XPS is used to detect the surface composition of supported metal oxide catalysts. The XPS signal is proportional to the surface metal oxide concentration in the first few layers that the signal penetrates. In the present study, the XPS signal of the surface rhenium and support cations was monitored. Based on the surface XPS signal, the ratios $(Re/S)_{XPS}$, where $S = Al$ or Ti, were determined. It is observed that the XPS ratios, $(Re/S)_{XPS}$, are always greater than

Fig. 8 Raman spectra of sodium doped Re_2O_7/Al_2O_3. Spectra obtained under dehydrated conditions.

$(Re/S)_{bulk}$, which suggests that the surface is enriched with rhenium. Furthermore, the linear increase in $(Re/S)_{XPS}$ with coverage is in accordance with the model by Kerkof and Moulijn,[47] suggesting the presence of well dispersed surface species. A similar increase in the surface XPS signal is also observed for supported rhenium oxide,[47] vanadium oxide,[41] tungsten oxide[41] and chromium oxide catalysts.[48,49] For supported vanadium oxide, tungsten oxide, molybdenum oxide and chromium oxide catalysts, the surface atom/support cation ratio increases linearly and then attains a relatively constant value above monolayer limits due to crystallite formation. For supported rhenium oxide samples, however, crystallites of rhenium oxide are never formed since Re_2O_7 volatilizes at the calcination temperatures used. The difference in the slope of the $(Re/Al)_{XPS}$ and $(Re/Ti)_{XPS}$ vs. $(Re/S)_{bulk}$ lines is probably related to the number of Al and Ti atoms present per unit volume, provided that the analysis volumes in the two samples are equal. Indeed, based on the unit cell dimensions, the number of Ti atoms is less than the number of Al atoms per unit volume. Thus, the XPS studies suggest that the rhenium oxide species is present as a well-dispersed surface species in the various supported rhenium oxide samples.

Raman and IR spectroscopy. Raman and IR spectroscopy are powerful techniques for studying the structure of the rhenium oxide species in supported rhenium oxide catalysts. Of the two types of vibrational spectropy, Raman is well suited for characterization since the spectra are less affected by the oxide support.[24] The assignments of the Raman bands present in the various spectra are made by comparing the spectra with those of reference compounds.

A stick diagram for some of the rhenium oxide reference compounds is given in Fig. 10.[22,24] The perrhenate ion in aqueous solution has a perfect ReO_4^- type tetrahedral structure with symmetric, asymmetric and bending vibrations at 971, 916 and 332 cm^{-1}, respectively. For tetrahedrally coordinated molecules confined to a crystalline lattice, the symmetry is lower than tetrahedral. Solid $NaReO_4$, having an S_4 symmetry, is such an example and possesses Raman bands at 963, 928, 890, 369 and 331 cm^{-1}. ReO_3F, with a C_{3v} symmetry, and ReF_3O_2, with a C_{2v} symmetry, are four and five coordinated rhenium oxide compounds possessing Raman bands at

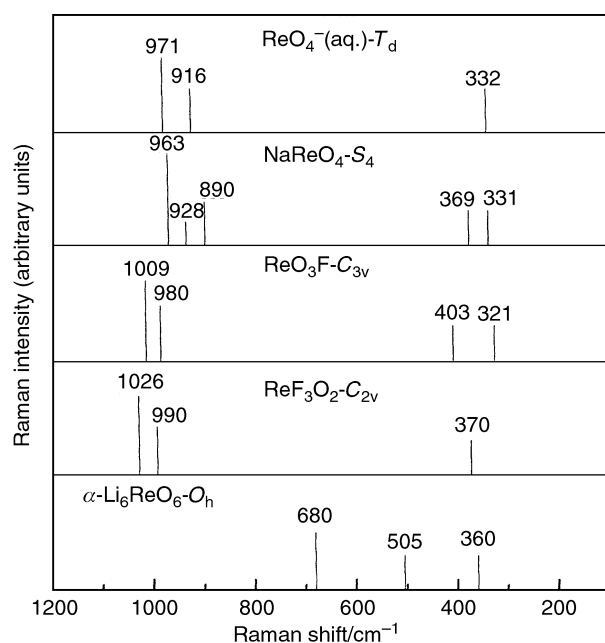1009, 980, 403, 321 cm^{-1} and 1026, 990, 370 cm^{-1}, respectively. α-Li_6ReO_6 has an ideal ReO_6 type octahedral structure with three of the fundamental modes active at 680, 505 and 360 cm^{-1}.

Dehydrated conditions. Under dehydrated conditions a distinct band is observed at ~ 1000 cm^{-1} for the rhenium oxide species on Al_2O_3 and TiO_2. For both sets of samples, the intensity of this Raman band at ~ 1000 cm^{-1} increases almost linearly with increasing rhenium content, which suggests that the same functionality is present on these oxide supports. An additional peak at 973 cm^{-1} is observed for >10% Re_2O_7 loading on Al_2O_3, which is assigned to the asymmetric vibration of the terminal Re=O bonds.[24] However, since the asymmetric vibrations are inherently weaker in the Raman spectra than the IR spectra, the 973 cm^{-1} Raman band may not be clearly observed in all samples. Indeed, the first overtone band at 1954–1974 cm^{-1} is observed in the IR spectra of all samples. In the IR spectra the first overtone region is monitored. The bands in the first overtone region of the Re=O vibration for the dehydrated IR spectra reveal the presence of bands at 1992–2003 and 1954–1974 cm^{-1} regions. The presence of the bands at 1992–2003 and 1954–1974 cm^{-1} is independent of the rhenium oxide loading and oxide support. Comparison of the Raman and IR spectra of Re_2O_7/Al_2O_3 and Re_2O_7/TiO_2 samples reveals that the same vibrational bands are present. The similar Raman and IR spectra of the Re_2O_7/Al_2O_3 and Re_2O_7/TiO_2 samples suggest that under dehydrated conditions the same type of surface rhenium oxide species is present on both supports.

The ~ 1000 cm^{-1} band that is present for all loadings is assigned to a terminal Re=O bond.[24] Since this bond is present at all loadings and for all supports, the same Re=O functionality is present on the oxide support surface. Furthermore, there is an absence of Raman bands at ~ 450 cm^{-1} and in the 200–150 cm^{-1} region, characteristic of Re–O–Re linkages, suggesting that the surface rhenium oxide species are isolated. Comparing the spectra with that of α-Li_6ReO_6 (given in Fig 10), which has an octahedral (six) coordinated rhenium oxide species, suggests that the surface species is not octahedral since no peak is observed at 680 cm^{-1}. Hence it appears that the surface rhenium oxide species is either four or five coordinated, isolated and possesses one or more Re=O functionalities.

The Raman and IR spectra also show that the vibration at 1000 cm^{-1} is both Raman and IR active, suggesting that the symmetry is lower than tetrahedral, and, consequently, possess either a C_{3v} or C_{2v} symmetry. The presence of a C_{2v} or C_{3v} symmetry depends on whether two or three of Re=O terminal bonds are present. Furthermore, the presence of symmetric and asymmetric bands also suggests that more than a single terminal Re=O bond exists for the surface rhenium oxide species. In order to ascertain whether the surface rhenium oxide species has a C_{3v} (three terminal Re=O bonds) or a C_{2v} (two terminal Re=O bonds) symmetry the Raman spectrum is compared with those of reference compounds. With arguments similar to those of Vuurman et al.,[24] the Raman spectra of the Re_2O_7/TiO_2 and Re_2O_7/Al_2O_3 catalysts suggest that the surface rhenium oxide species possesses three Re=O terminal bonds. Thus, combined information from Raman and IR spectroscopy implies that the surface rhenium oxide species is isolated and four coordinated with C_{3v} symmetry (three terminal Re=O bonds).

Recent developments in ^{18}O exchange experiments over supported rhenium oxide catalysts, however, indicate the presence of a single terminal Re=O bond.[50] This observation suggests that more than one type of surface rhenium oxide species is present on the oxide support since Raman bands corresponding to bridging Re–O–Re are absent. Despite this apparent discrepancy, it appears that similar surface rhenium oxide

Fig. 10 Raman bar diagram for some rhenium oxide compounds in different coordinations.

species are present on the oxide support since the Raman and IR spectra are similar.

Temperature programmed reduction studies. TPR is a valuable technique for investigating the reducibility of rhenium catalysts. In the present study the consumption of hydrogen was monitored as the temperature was increased linearly with time. By using this method, the ease with which the oxygen is removed from the catalyst is analyzed. Thus, if the temperature of the reduction peak is lower, then a higher reducibility of the catalyst is suggested. Detailed information about reducibility is critical because reduction of the surface rhenium oxide species is important during redox reactions. Furthermore, in some cases, the catalytically active rhenium sites are created by the reduction of surface Re^{7+} oxide present on the freshly prepared catalyst.

It was observed that the reduction peaks for each of the Re_2O_7/Al_2O_3 and Re_2O_7/TiO_2 samples are distinct. When the reduction peaks of the Re_2O_7/Al_2O_3 and Re_2O_7/TiO_2 samples are plotted *vs.* rhenium oxide loading (Fig. 2), two distinct regions of reduction peaks are observed. It is also evident from the plot that for both sets of samples the reduction peak remains relatively constant at $\sim 217\,^\circ C$ (Re_2O_7/TiO_2) and $\sim 352\,^\circ C$ (Re_2O_7/Al_2O_3) for different rhenium oxide loadings. This difference in temperature for the rhenium oxide species reduction on different supports suggests that the oxygen bonding is different for the two sets of catalysts. Based on the structural studies from vibrational spectroscopy, there are essentially two types of oxygen species present: the terminal Re=O oxygen and the bridging Re–O–support oxygen. Since the Raman spectra of both Re_2O_7/TiO_2 and Re_2O_7/Al_2O_3 catalysts show bands at ~ 1000 cm^{-1} due to the terminal Re=O bond, the terminal Re=O bond strengths for both sets of samples are, therefore, similar. Consequently, the TPR studies suggest that the difference in bonding energy of the oxygen species is due to differences in the Re–O–support bond strength. The reduction peak for the Re_2O_7/TiO_2 samples is lower than that of the Re_2O_7/Al_2O_3 samples. Hence the reducibility of the titania supported samples is greater than that of the alumina supported samples. This is in agreement with the trend observed by Vuurman *et al.*[24] The Re–O–support bond is, therefore, stronger for the alumina than the titania support.

In summary, spectroscopic characterization of the Re_2O_7/TiO_2 and Re_2O_7/Al_2O_3 samples suggest that the same surface rhenium oxide species is present on both oxide supports. However, the behavior of the surface rhenium oxide species under reduction environments strongly depends on the specific oxide support, as demonstrated by the TPR experiments. This reduction behavior appears to be related to the strength of the bridging Re–O–support bond rather than the terminal Re=O bond.

Effect of additives

The effect of vanadium and sodium additives on the surface rhenium oxide species was investigated. The Raman spectra of the unmodified V_2O_5/TiO_2 and Re_2O_7/TiO_2 samples under dehydrated conditions show that the V=O vibration is at 1026 cm^{-1} whereas that for Re=O vibration is at ~ 1003 cm^{-1}. The Re_2O_7/TiO_2 samples modified with surface vanadium oxide show Raman features similar to the Re_2O_7/TiO_2 sample (band at 1002 cm^{-1}), suggesting that the same surface rhenium oxide species is present. The presence of the surface vanadium oxide species is confirmed by the shoulder at ~ 1025 cm^{-1} in the Raman spectra of these samples. The TPR data for surface vanadium oxide modified Re_2O_7/TiO_2 and Re_2O_7/Al_2O_3 samples show that the addition of surface vanadium oxide results in a slight shift of the reduction peak to higher values. The single sharp reduction peak is retained and

there are no other significant reduction peaks. Hence the results of Raman and TPR studies demonstrate that the presence of vanadium oxide species in the vanadia modified Re_2O_7/Al_2O_3 and Re_2O_7/TiO_2 samples does not affect the structure of the surface rhenium oxide species, but coordinates to the support directly. Furthermore, there is no compound formation between the surface vanadium oxide and the rhenium oxide species since the Raman intensity of the surface rhenium oxide species is maintained. The surface vanadium oxide can be said to be a non-interacting additive for the Re_2O_7/Al_2O_3 and Re_2O_7/TiO_2 samples.

The addition of sodium has a more pronounced effect on the surface rhenium oxide species, as is evident from the dehydrated Raman spectra of these samples. The addition of sodium results in a noticeable decrease in the Re=O Raman band position, which is due to an increase in the Re–O bond length. This decrease in Raman band position is especially true for the 1, 2 and 3% $Na_2O/3.1\%$ Re_2O_7/TiO_2 and 5 and 10% $Na_2O/7.8\%$ Re_2O_7/Al_2O_3 samples. The 1% $Na_2O/7.8\%$ Re_2O_7/Al_2O_3 sample, however, does not show a significant change since an appreciable part of Al_2O_3 is still exposed, and it appears that the sodium coordinates with the exposed Al_2O_3 sites. In addition, the Na/Re ratio is small (see Table 2), which is not sufficient to affect a change in the Raman spectra of the surface rhenium oxide species. Furthermore, comparison of ambient and dehydrated Raman spectra of the sodium modified supported rhenium oxide samples suggests compound formation for the samples possessing Na/Re atomic ratios > 2 since the Raman bands at 950–970, ~ 920 and ~ 888 cm^{-1} (in the 700–1200 cm^{-1} region) are not affected by dehydration. Not surprisingly, these Raman band positions are similar to those for compounds containing sodium and rhenium oxide, $NaReO_4$, discussed above and given in Fig. 10, where the Na/Re atomic ratio = 1.

The effect of sodium on the surface rhenium oxide species is also evident from the TPR experiments. Addition of sodium to the Re_2O_7/Al_2O_3 and Re_2O_7/TiO_2 samples results in a shift of the reduction peak to higher temperatures. For all the sodium modified Re_2O_7/TiO_2 samples the reduction peak is between 400 and 430 $^\circ C$. Similarly, for 5 and 10% $Na_2O/7.8\%Re_2O_7/Al_2O_3$ samples the reduction peak is between 400 and 410 $^\circ C$. The 1% $Na_2O/7.8\%Re_2O_7/Al_2O_3$ sample, however, has a reduction peak at 380 $^\circ C$, which suggests that the surface rhenium oxide species is not significantly affected for this low level of sodium. This is in line with the Raman studies discussed above, where the sodium does not significantly affect the Raman spectra of the 1% $Na_2O/7.8\%Re_2O_7/Al_2O_3$ sample. It appears from the Raman and TPR studies that low sodium coverages do not significantly affect the structure or reducibility of the surface rhenium oxide species. Hence sodium, when present in appreciable amounts (Na/Re atomic ratio > 2) can be said to be an interacting additive and acts as a redox poison towards the surface rhenium oxide species since it significantly affects its structure and reduction characteristics.

Similar interactions of metal oxide additives with supported vanadium oxide catalysts were observed previously.[40] The surface vanadium oxide species in these catalysts are not significantly affected by the presence of non-interacting additives of WO_3, SiO_2 and Nb_2O_5, but are affected by interacting additives such as K_2O and P_2O_5.

Conclusions

The nature of the surface rhenium oxide species was determined using various characterization techniques as a function of oxide supports (Al_2O_3 and TiO_2), rhenium oxide loading and metal oxide additives (vanadium and sodium). The characterization techniques used were X-ray photoelectron, Raman and FTIR spectroscopy and TPR.

The XPS studies suggest that the surface rhenium oxide species are well dispersed on the oxide support. The vibrational spectra of the surface rhenium oxide species on the support were determined under dehydrated conditions using Raman and FTIR spectroscopy. Under dehydrated conditions, two distinct rhenium oxide vibrational bands were observed independent of the oxide support and rhenium oxide loading. Analysis of the vibrational spectra suggests that similar rhenium oxide species are present independent of the oxide support and rhenium oxide loading. Work is in progress to elucidate the exact structure of the surface rhenium oxide species.

TPR studies revealed that the reduction peak in hydrogen was independent of rhenium oxide loading, but strongly dependent on the specific oxide support. The reducibility of the Re_2O_7/TiO_2 catalysts was more efficient than that of the Re_2O_7/Al_2O_3 catalysts, as indicated by the hydrogen reduction peak for the Re_2O_7/TiO_2 catalysts at $\sim 217\,^{\circ}C$. Complete reduction of the surface rhenium oxide species occurred, from Re^{7+} to Re^0, irrespective of the oxide support and rhenium oxide loading. Furthermore, from TPR studies it appears that the strength of the bridging Re–O–support bond is stronger for Al_2O_3 than for TiO_2.

The effect of surface metal oxide additives was studied by addition of vanadium and sodium to the Re_2O_7/TiO_2 and Re_2O_7/Al_2O_3 samples. The results of the Raman and TPR studies suggested that there are two types of interactions between the additives and the surface rhenium oxide species. Vanadium acts as a non-interacting additive by directly binding to the oxide support and not significantly affecting the structure and reducibility of the surface rhenium oxide species on TiO_2 and Al_2O_3. Substantial amounts of sodium (Na/Re atomic ratio > 2), however, act as an interacting additive by directly coordinating with the surface rhenium oxide species and, thereby, changing its structure and reducibility.

Acknowledgement

References

1 J. R. Bartlett and R. P. Cooney, in *Spectroscopy of Inorganic-based Materials*, ed. R. J. H. Clark and R. E. Hester, Wiley, New York, 1987, p. 187
2 F. D. Hardcastle and I. E. Wachs, in *Proceeding of the 9th International. Congress on Catalysis*, ed. M. S. Phillips and M. Ternan, Chemical Institute of Canada, Ontario, 1988, vol. 4, p. 1449.
3 *Catal. Today*, 1999, **51**(2), 201 (special issue, ed. I. E. Wachs).
4 C. L. Thomas, *Catalytic Processes and Proven Catalysis*, Academic Press, New York, 1970.
5 J. C. Mol and J. A. Moulijn, *Adv. Catal.*, 1975, **24**, 131.
6 J. C. Mol, *Catal. Today*, 1999, **51**, 289.
7 A. A. Olsthoorn and C. Boelhouwer, *J. Catal.*, 1976, **44**, 207.
8 J. C. Mol, *J. Mol. Catal.*, 1982, **15**, 35.
9 J. Hietala, A. Root and P. Knuuttila, *J. Catal.*, 1994, **150**, 46.
10 T. A. Pecoraro and R. R. Chianelli, *J. Catal.*, 1981, **67**, 430.
11 R. Thomas, E. M. van Oers, V. H. J. de Beer, J. Medema and J. A. Moulijn, *J. Catal.*, 1982, **76**, 241.
12 E. W. Stern, *J. Catal.*, 1979, **57**, 390.
13 W. H. Davenport, V. Kollonitsch and C. Kline, *Ind. Eng. Chem.*, 1968, **60**, 11.
14 I. E. Wachs, G. Deo, A. Andreini, M. A. Vuurman and M. de Boer, *J. Catal.*, 1996, **160**, 322.
15 I. E. Wachs, G. Deo, D. S. Kim, M. A. Vuurman and H. Hu, *J. Mol. Catal.*, 1993, **83**, 443.
16 X. Xiaoding, P. Imhoff, G. C. N. van der Aardweg and J. C. Mol, *J. Chem. Soc., Chem. Commun.*, 1985, 273.
17 X. Xiaoding and J. C. Mol, *J. Chem. Soc., Chem. Commun.*, 1985, 631.
18 A. Andreini, X. Xiaoding and J. C. Mol, *Appl. Catal.*, 1986, **27**, 31.
19 X. Xiaoding, C. Boelhouwer, J. I. Benecke, D. Vonk and J. C. Mol, *J. Chem. Soc., Faraday Trans. 1*, 1986, **82**, 1945.
20 K. P. J. Williams and K. Harrison, *J. Chem. Soc., Faraday Trans.*, 1990, **86**, 1603.
21 A. Ellison, G. Diakun and P. Worthington, *J. Mol. Catal.*, 1988, **46**, 131.
22 F. D. Hardcastle, I. E. Wachs, J. A. Horsley and G. H. Via, *J. Mol. Catal.*, 1988, **46**, 15.
23 L. Wang and W. K. Hall, *J. Catal.*, 1983, **82**, 177.
24 M. A. Vuurman, I. E. Wachs, D. J. Stufkens and A. Oskam, *J. Mol. Catal.*, 1992, **76**, 263.
25 T. Kawai, K. M. Jiang and T. Ishikawa, *J. Catal.*, 1996, **159**, 288.
26 F. P. J. M. Kerkhof, J. A. Moulijn and R. Thomas, *J. Catal.*, 1979, **56**, 279.
27 D. S. Kim and I. E. Wachs, *J. Catal.*, 1993, **141**, 419.
28 W. N. Delgass, G. L. Haller, R. Kellerman and J. H. Lunsford, *Spectroscopy in Heterogeneous Catalysis*, Academic Press, New York, 1979.
29 S. S. Chan, I. E. Wachs, L. L. Murrell, L. Wang and W. K. Hall, *J. Phys. Chem.*, 1984, **88**, 5831.
30 E. S. Shpiro, V. I. Avaev, G. V. Antoshin, M. A. Ryashentseva and K. M. Minachev, *J. Catal.*, 1978, **55**, 402.
31 L. G. Duquette, R. C. Cieslinski, C. W. Jung and P. E. Garrou, *J. Catal.*, 1984, **90**, 362.
32 R. M. Edreva-Kardjieva and A. A. Andreev, *J. Catal.*, 1985, **94**, 97.
33 R. M. Edreva-Kardjieva and A. A. Andreev, *J. Catal.*, 1986, **97**, 321.
34 X. Yide, H. Jiasheng, L. Zhiying and G. Xiexian, *J. Mol. Catal.*, 1991, **65**, 275.
35 H. C. Yao and M. Shelef, *J. Catal.*, 1976, **44**, 392.
36 P. Arnoldy, E. M. van Oers, O. S. L. Bruinsma, V. H. J. de Beer and J. A. Moulijn, *J. Catal.*, 1985, **93**, 231.
37 P. Arnoldy, O. S. L. Bruinsma and J. A. Moulijn, *J. Mol. Catal.*, 1985, **30**, 111.
38 G. Deo and I. E. Wachs, *J. Catal.*, 1994, **146**, 323.
39 N. Arora, G. Deo, I. E. Wachs and A. M. Hirt, *J. Catal.*, 1996, **159**, 1.
40 J.-M. Jehng, G. Deo, B. K. Weckhuysen and I. E. Wachs, *J. Mol. Catal. A: Chem.*, 1996, **110**, 41.
41 M. A. Vuurman, I. E. Wachs and A. M. Hirt, *J. Phys. Chem.*, 1991, **95**, 9928.
42 L. Burcham and I. E. Wachs, *Catal. Today*, 1999, **49**, 467.
43 A. M. Turek, I. E. Wachs and E. DeCanio, *J. Phys. Chem.*, 1992, **96**, 5000.
44 J. Okal, L. Kepinski, L. Krajczyk and M. Drozd, *J. Catal.*, 1999, **188**, 140.
45 G. Deo and I. E. Wachs, *J. Catal.*, 1994, **140**, 335.
46 I. R. Beattie and T. R. Gilson, *J. Chem. Soc. A*, 1969, 2322.
47 F. P. J. M. Kerkhof and J. A. Moulijn, *J. Phys. Chem.*, 1979, **83**, 1612.
48 Ch. Fountzoula, H. K. Matralis, Ch. Papadopoulo, G. A. Voyiatzis and Ch. Kordulis, *J. Catal.*, 1997, **172**, 391.
49 M. Cherian, A. M. Hirt and G. Deo, unpublished results.
50 B. M. Weckhuysen, J-M. Jehng and I. E. Wachs, in preparation.